


Article

Environmental Controls of Diurnal and Seasonal Variations in the Stem Radius of *Platycladus orientalis* in Northern China

Manyu Dong ^{1,2} , Bingqin Wang ², Yuan Jiang ^{1,2,*} and Xinyuan Ding ²¹ State Key Laboratory of Earth Surface Process and Resource Ecology, Beijing Normal University, Beijing 100875, China² Faculty of Geographical Science, Beijing Normal University, Beijing 100875, China

* Correspondence: jiangy@bnu.edu.cn; Tel.: +86-010-5880-6093

Received: 7 August 2019; Accepted: 6 September 2019; Published: 9 September 2019



Abstract: Fine-resolution studies of stem radial variation over short timescales throughout the year can provide insight into intra-annual stem dynamics and improve our understanding of climate impacts on tree physiology and growth processes. Using data from high-resolution point dendrometers collected from *Platycladus orientalis* (Linn.) trees between September 2013 and December 2014, this study investigated the daily and seasonal patterns of stem radial variation in addition to the relationships between daily stem radial variation and environmental factors over the growing season. Two contrasting daily cycle patterns were observed for warm and cold seasons. A daily mean air temperature of 0 °C was a critical threshold that was related to seasonal shifts in stem diurnal cycle patterns, indicating that air temperature critically influences diurnal stem cycles. The annual variation in *P. orientalis* stem radius variation can be divided into four distinct periods including (1) spring rehydration, (2) the summer growing season, (3) autumn stagnation, and (4) winter contraction. These periods reflect seasonal changes in tree water status that are especially pronounced in spring and winter. During the growing season, the maximum daily shrinkage (MDS) of *P. orientalis* was positively correlated with air temperature (T_a) and negatively correlated with soil water content (SWC) and precipitation (P). The vapor pressure deficit (VPD) also exhibited a threshold-based control on MDS at values below or above 0.8 kPa. Daily radial changes (DRC) were negatively correlated with T_a and VPD but positively correlated with relative air humidity (RH) and P. These results suggest that the above environmental factors are associated with tree water status via their influence on moisture availability to trees, which in turn affects the metrics of daily stem variation including MDS and DRC.

Keywords: *Platycladus orientalis* (Linn.); stem radial variation; daily and seasonal patterns; growing season; environmental factors

1. Introduction

A complete assessment of the response of tree growth to climates over different time scales is critical for understanding the physiological mechanisms of tree growth and their response to environments in the context of global climate change [1]. Long-term relationships between tree radial growth and climatic variables have been evaluated in recent decades by mostly using dendrochronological approaches that are based on the statistical relationships between tree-ring widths and meteorological factors at monthly, seasonal, and annual scales [2,3]. However, these approaches do not allow one to study the effects of short-term environmental changes on tree growth at intra-annual scales. Thus, studies applying fine-resolution growth data complement longer-term, tree ring-based studies [4–6].

Variation in tree stem diameter results from irreversible growth due to new cambial cell formation only during the growing season and reversible stem shrinkage and swelling associated with water

balance within the stems [7,8]. Generally, a stem contracts during the daytime when tree transpiration exceeds water absorption via the roots and expands at night due to excess absorption from the roots with respect to transpiration [9]. Dendrometers continuously and automatically monitor intra-annual stem radial variation at a high temporal resolution of minutes to hours without invasive sampling [10–12]. Such technology has provided opportunities to study stem radial variation and its response to environmental factors on daily and seasonal scales [3,7]. Consequently, this method has been widely used in recent years to investigate intra-annual stem radial variation and evaluate growth-climate relationships in various ecosystems [8,13–16]. At the daily scale, two opposing patterns of diurnal cycles of stem radial variations are observed in warm and cold seasons that are related to the physiological processes of transpiration and water uptake, and freeze-thaw cycles, respectively [17–19]. Nevertheless, it is unclear which environmental factors affect seasonal shifts of stem diurnal cycle patterns and what the corresponding thresholds are. Turcotte et al. [20] identified the stem radial variation corresponding to three seasonal periods for black spruce in the southern boreal forest of Quebec, Canada. These periods were related to winter shrinkage, spring rehydration, and summer transpiration. Other studies have shown that intra-annual stem radial variation exhibits a bimodal distribution in Mediterranean trees [21] and S-shaped curves in tropical regions [22]. These observations reflect that seasonal patterns of intra-annual stem radial variation are differentiated among different climatic regions. The widely used metrics, daily radial change (DRC) and maximum daily shrinkage (MDS), are provided by dendrometer measurements and yield valuable data to determine seasonal tree growth and tree water status, thereby allowing the investigation of relationships between stem radial variation and environmental variables [23–26]. Liu et al. [5] reported that the MDS values of *Larix principis-rupprechtii* in northern China are mainly influenced by air temperatures over the entire growing season. In addition, Oberhuber et al. [27] observed that DRC values of *Pinus sylvestris* (L.) Karst., *Larix decidua* Mill., and *Picea abies* L. trees were directly correlated with relative air humidity and precipitation and indirectly correlated with vapor pressure deficit (VPD) and air temperatures.

Platykladus orientalis (Linn.) is an evergreen tree species that originated in China and exhibits well-developed root systems and long lifespans [11]. The trees are able to endure severe drought and persist on barren soils and are thus commonly used for ecological restoration in arid mountain landscapes of northern China [28]. The environment–growth relationships of *P. orientalis* have been investigated by several recent dendroclimatological studies within northern China at the annual scale [29,30]. However, investigations of intra-annual stem radial variation in *P. orientalis* over a yearly cycle are scarce. In one such study, Jiang et al. [8] investigated the response of *P. orientalis* daily stem radial increments to environmental factors during the growing season. Investigation over this shorter timescale cannot however reflect the seasonal rhythm of stem radial variation over the whole year. To address this knowledge-gap, we evaluated the *P. orientalis* intra-annual stem radial variation and response of stem radial variation to weather in northern China using high-resolution point dendrometer data collected from September 2013 to December 2014. The main objectives of the study were to (1) determine the daily and seasonal patterns of stem radial variation in *P. orientalis*; (2) identify the major factors controlling seasonal shifts of stem diurnal cycle patterns; and (3) evaluate the relationships among DRC, MDS, and environmental factors over the growing season.

2. Materials and Methods

2.1. Study Area

This study was conducted in the Huailai Basin of the Hebei province in North China (Figure 1), which is one of the main distribution areas of the natural secondary forest of *P. orientalis* and is also located in the transition zone between arid and humid regions. *P. orientalis* is the dominant tree species within the forests at the study site and is commonly found on the tops and slopes of hills [11]. The regional climate is classified as temperate continental monsoonal and is characterized by cold and dry winters and hot and rainy summers. The average annual precipitation is 376 mm, of which

65% falls between June and August. The mean annual temperature is 9.6 °C, and July is the warmest month (mean: 24.5 °C), while January is the coldest month (−7.4 °C). A 30 m × 30 m plot (40°15′37.9″ N, 115°36′39.6″ E; 495 m a.s.l.) was established in 2013 within a pure *P. orientalis* forest, with good growth of trees and little anthropogenic influence. This area is located on a north-facing slope with a slope gradient of 18°. The soil texture at the study site is sandy loam, and the soil depth is 60 cm, with a maximum available soil water capacity up to 28%. As a shallow root plant, the root system of *P. orientalis* is mainly distributed between 0 and 50 cm of the soil layer.

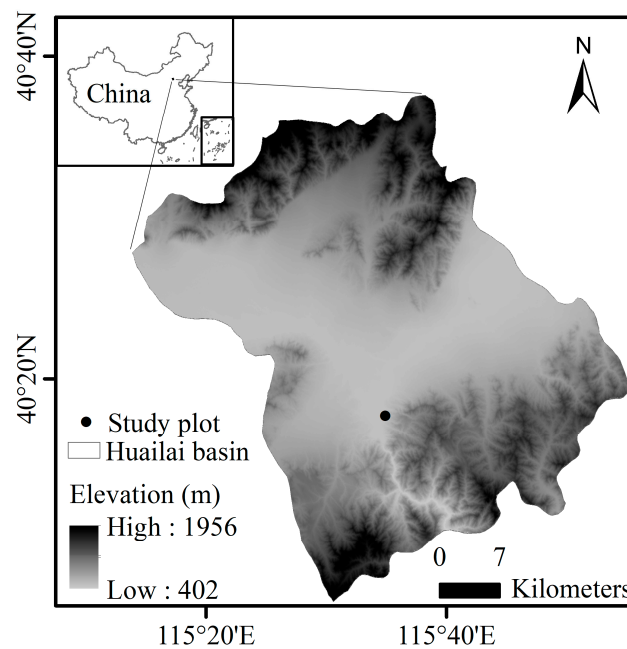


Figure 1. The location of the study site and study plot.

2.2. Dendrometer Measurements

Four healthy and upright trees with average growth characteristics (diameter at breast height (DBH), 7.5 ± 0.5 cm; tree height (H), 4.0 ± 0.4 m; tree ages, 40.5 ± 3.2 years) were selected for this study, which are close to the mean DBH (7.2 ± 1.2 cm) and H (3.6 ± 0.8 m) of the stand. High-resolution point dendrometers (Type DR, Ecomatik, Munich, Germany; accuracy <2 μm , temperature coefficient 0.1 lm/K) were installed in stems at 1.0–1.3 m height in an orientation perpendicular to the slope. To reduce the influence of hygroscopic expansion and contraction of the bark, the outermost bark layer was removed without wounding the cambial zone prior to installing the dendrometers [31]. Stem radial variations of the trees were automatically recorded on a data logger (DL 10, Ecomatik, Munich, Germany), from 1 September 2013 to 31 December 2014 at 30 min intervals. Measurements for the four trees were not recovered between 15 November and 6 December in 2013 due to instrument failures.

2.3. Meteorological Measurements

An automated weather station (HOBO, Onset, Pocasset, USA) was also installed on the north slope, where the local region was relatively flat, near the research site to collect weather data including air temperatures (T_a , °C), relative air humidity (RH, %), and precipitation (P, mm) at 2 m height. The volumetric soil water content (SWC, %; Em50, Decagon, Pullman, WA, USA) and soil temperature (T_s , °C; Em50, Decagon, Pullman, WA, USA) were monitored at 20 cm depth close to the experimental trees. Environmental factors were recorded at 30 min intervals to correspond with the dendrometer

measurements. The vapor pressure deficit (VPD, kPa) was calculated from T_a and RH using the Magnus equation [32]:

$$\text{VPD} = 6.10 \times e^{\frac{17.08 \times T_a}{234.2 + T_a}} \times \left(1 - \frac{\text{RH}}{100}\right). \quad (1)$$

2.4. Data Analysis

The daily stem mean value (R) was calculated as the average of 48 values of four sample trees measured by the dendrometers over one day. The DRC was defined as the difference between the mean values of two consecutive days (i.e., the “daily mean approach” [33]) and represents a combination of water- and growth-induced radius changes [34]. This method is simpler than the previously suggested cycle approach [35]. Moreover, Deslauriers et al. [33] determined that the daily mean approach provides results that are consistent with those from the stem cycle approach. The cumulative stem radial variation (CRV) was calculated as the cumulative DRC sum and represents seasonal variation patterns [20]. As for CRV, four sample trees have similar synchronous changes, and the regression determination coefficient (R^2) between any two sample trees is as high as 0.97. The MDS was calculated as the differences between the daily maximum and minimum values [19] and reflected the diurnal rhythms of water-storage depletion and replenishment [35]. On rare days when the stem size monotonically increased or decreased, no MDS values were assigned [18]. To investigate the stem diurnal cycles, the overall growth trend was removed from the data by calculating the daily means for each sensor and subtracting it from the measurements [18]; air temperature data were also processed in the same way. The stem’s mean diurnal curve for stages 1 and 2 was a mean over the four trees and the days within stages 1 and 2, respectively.

Kolmogorov–Smirnov tests were used to evaluate the normal distributions of environmental variable data [27] and indicated that the SWC and P data were not normally distributed. Thus, Kendall’s rank correlation (τ) was calculated between the SWC and P factors with MDS or DRC during the growing season, while the Pearson correlation coefficients (r) were calculated between other environmental factors (T_a , T_s , RH, and VPD) and MDS or DRC during the growing season [27]. Statistical analyses were conducted using the SPSS 17.0 software (SPSS Inc., Chicago, IL, USA).

3. Results

3.1. Environmental Conditions

Daily air temperature means (T_a) varied between -10.6 °C and 30.6 °C over the study period (Figure 2). Soil temperature (T_s) also closely followed air temperature, albeit with smaller amplitudes. The total precipitation was 304.4 mm in 2014, and frequent rainfall events in June and September resulted in high SWC values. The drought period occurred in mid–late May and July–August, with SWC generally below 10% and T_a above 20 °C. The VPD varied widely with strong fluctuations, and the highest value (3.0 kPa) occurring in late May. Daily RH varied between 17.6% and 100%, with an average of 56.3%.

3.2. Diurnal Stem Cycles

The diurnal cycles of stem radius for *P. orientalis* were compared against the within-day air temperatures from 1 September 2013 to 31 December 2014 (Figure 3). The correlation coefficients clearly changed over time, with two distinct stages. During stage 1, the daily mean air temperature was <0 °C, and diurnal stem cycles were primarily positively correlated with air temperatures. The negative relationships during stage 1 were related to large increases in air temperature reaching approximately 0 °C. However, stage 2 was characterized by negative relationships between the two above values, when daily mean air temperatures were >0 °C. Positive relationships during stage 2 were related to large stem increases due to precipitation. The threshold between the two stages corresponded with the timing of daily mean air temperatures, reaching 0 °C. Due to instrument failures, the stem

radial variation in December 2013 was unfortunately not entirely recovered when daily mean air temperatures were 0 °C.

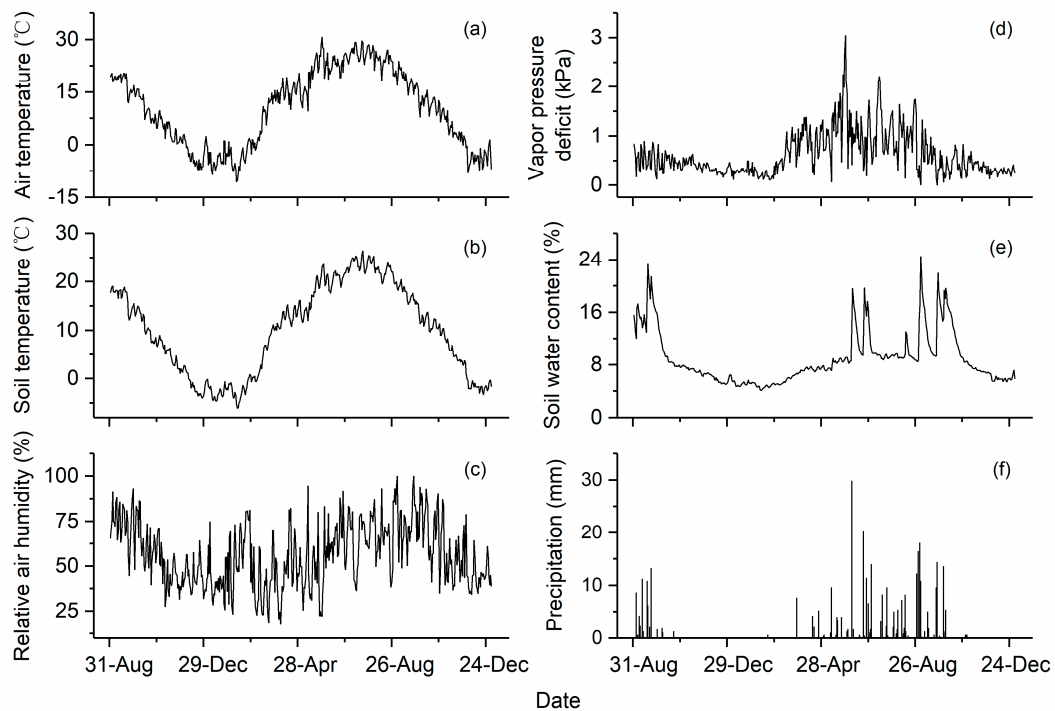


Figure 2. Daily climatic conditions at the study site from 1 September 2013 to 31 December 2014. (a) Mean daily air temperature (T_a); (b) mean daily soil temperature (T_s); (c) relative air humidity (RH); (d) vapor pressure deficit (VPD); (e) soil water content (SWC); and (f) Precipitation (P).

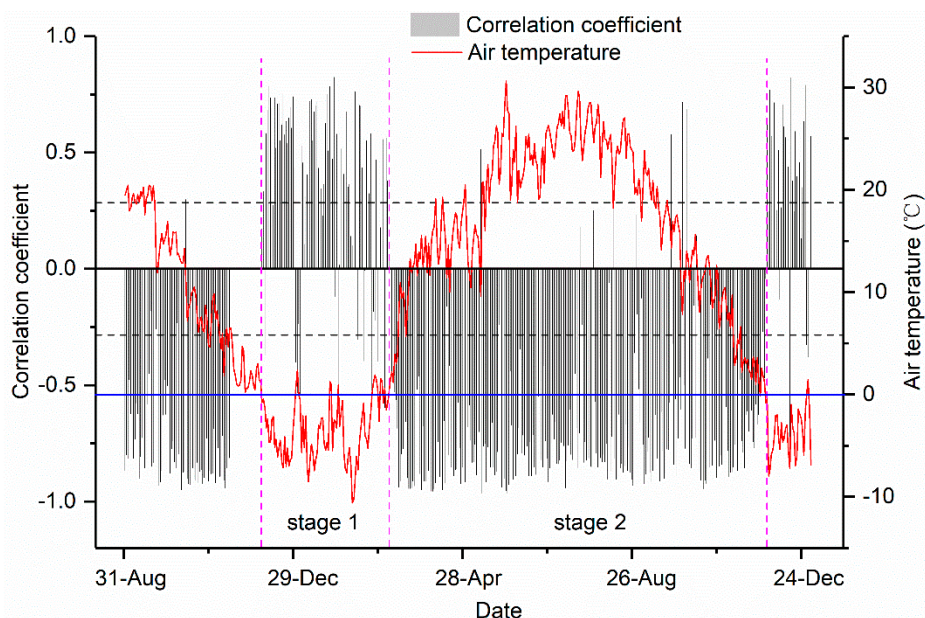


Figure 3. Pearson correlation coefficients between diurnal stem cycles and within-day air temperatures. Vertical dashed line corresponds to stage partition times of 24 March and 30 November. Horizontal dotted lines indicate $p = 0.05$ statistical significance threshold values.

The stem mean diurnal curve was generally synchronous with air temperature during stage 1 (Figure 4), although stem changes were slightly delayed by 2–3 h. During stage 2, the diurnal stem cycle curve exhibited an opposing trend as the temperature change curve, albeit with a 1 h lag time.

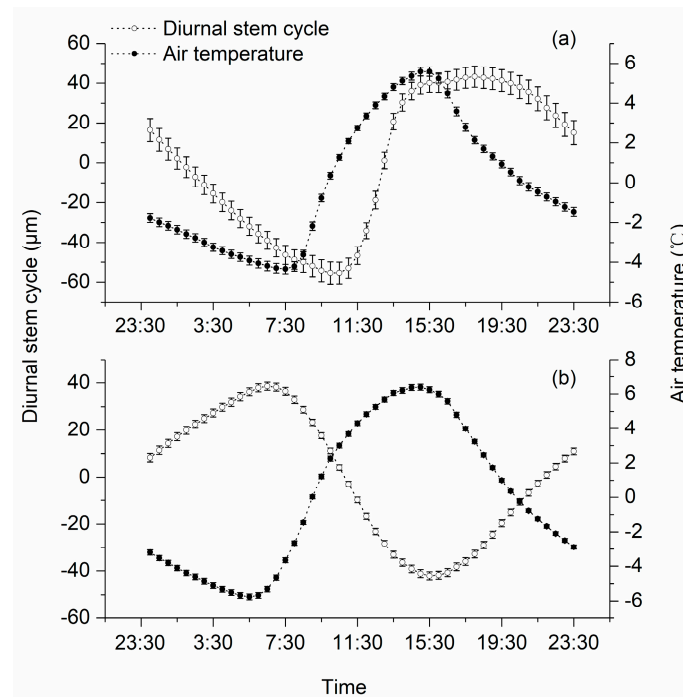


Figure 4. Mean diurnal cycles of stem radius and air temperature changes over stages (a) 1 and (b) 2. Error bars indicate standard error.

3.3. Seasonal Stem Radial Variation

The seasonal dynamics of the cumulative *P. orientalis* stem radial variation compared against air and soil temperatures yielded distinct patterns (Figure 5). Clear seasonal variation patterns could be distinguished among four distinct periods corresponding to spring rehydration (phase A), the summer growing season (phase B), autumn stagnation (phase C), and winter contraction (phase D). During the growing season (phase B), MDS widely fluctuated, with values ranging between 22.2 and 228.3 μm . DRC values increased with large fluctuations during the growing season, with most negative values occurring during drought periods in mid-late May and July–August.

3.4. Relationships between the Daily Stem Radial Variation and Environmental Factors during Growing Season

The daily stem radial variation (MDS and DRC values) of *P. orientalis* was investigated in relation to environmental factors during the growing period (Figures 6 and 7). MDS was linearly related to T_a ($r = 0.25$ $p < 0.001$) and inversely related to SWC ($\tau = -0.12$ $p < 0.05$) and P ($\tau = -0.19$ $p < 0.01$). The relationship between MDS and VPD was somewhat complex, necessitating a piecewise regression based on the R package “Segmented” to identify a threshold value of 0.8 kPa along the VPD gradient. When VPD was below and above 0.8 kPa, the correlation coefficients between MDS and VPD were 0.54 ($p < 0.001$) and -0.30 ($p < 0.01$), respectively. Relationships were not significant between MDS and T_s and RH. In contrast, DRC was linearly correlated with P ($\tau = 0.32$ $p < 0.001$) and RH ($r = 0.38$ $p < 0.001$). Significant inverse relationships were also observed between DRC and T_a ($r = -0.23$ $p < 0.01$) and VPD ($r = -0.43$ $p < 0.001$). Correlations between DRC and T_s and SWC were not statistically significant.

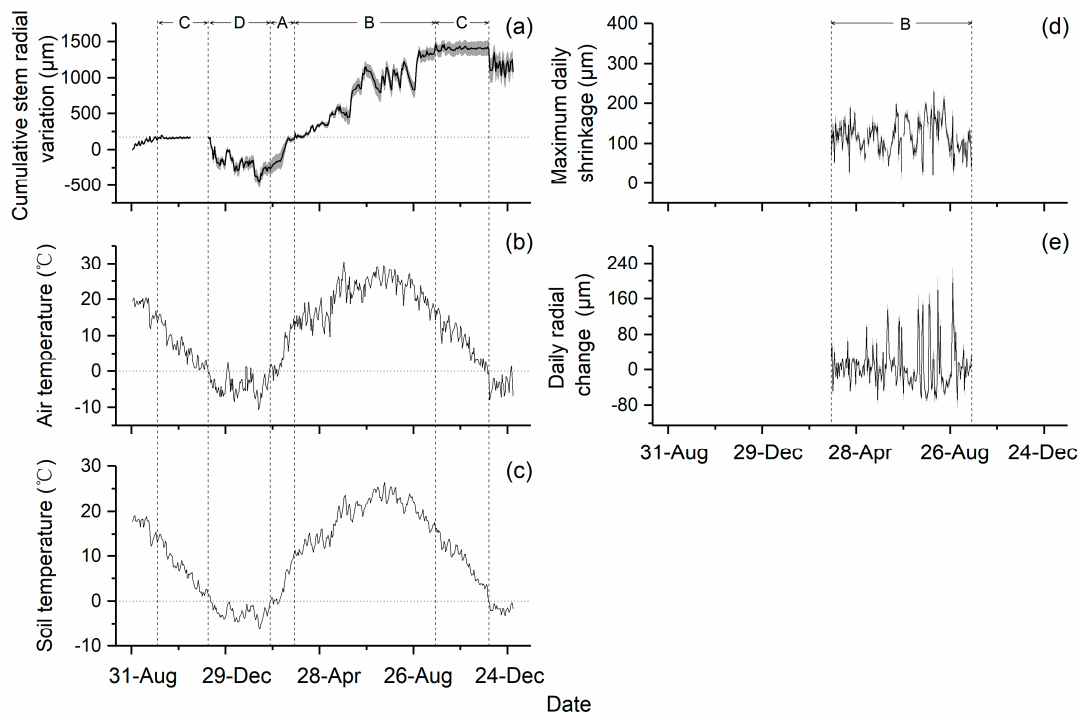


Figure 5. Daily time series of cumulative stem radial variation (CRV) (a), air temperature (b), soil temperature (c), maximum daily shrinkage (MDS) (d), and daily radial change (DRC) (e); the four distinct growth periods of *P. orientalis* radial change corresponding to spring rehydration (phase A), the summer growing season (phase B), autumn stagnation (phase C), and winter contraction (phase D). The standard errors for CRV, MDS, and DRC are indicated by the shaded areas around the black lines.

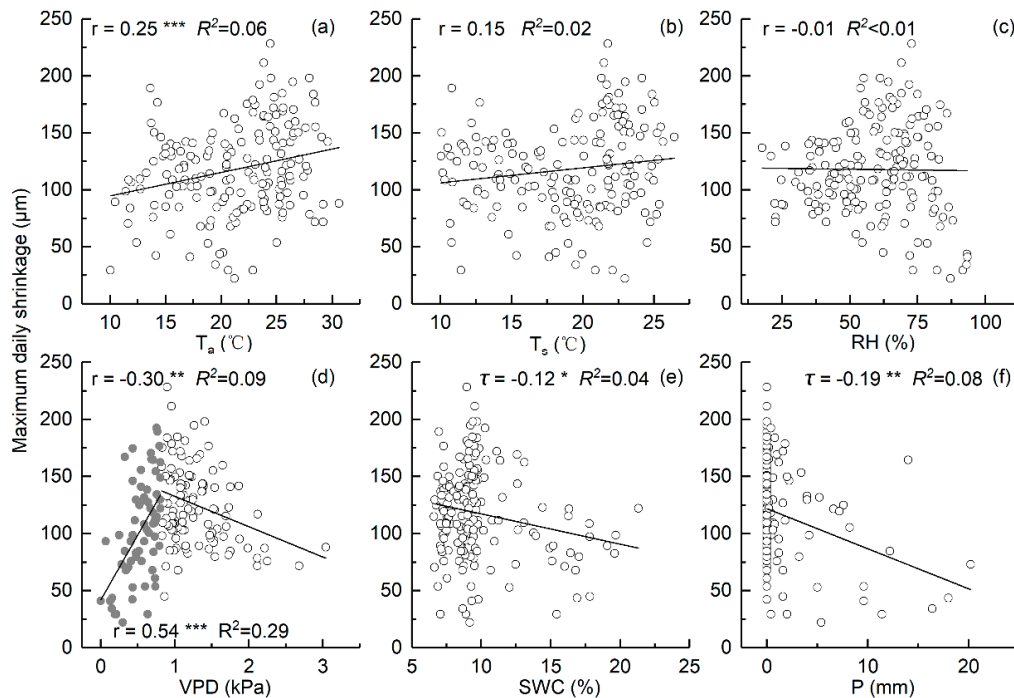


Figure 6. Correlations between MDS of *P. orientalis* and environmental factors of T_a (a), T_s (b), RH (c), VPD (d), SWC (e), and P (f) during growing season. Pearson correlation coefficient (r) values and Kendall’s tau coefficient (τ) values are shown with *: $p < 0.05$, **: $p < 0.01$, ***: $p < 0.001$. The gray and white dots in (d) indicate VPD values below and above 0.8 kPa, respectively.

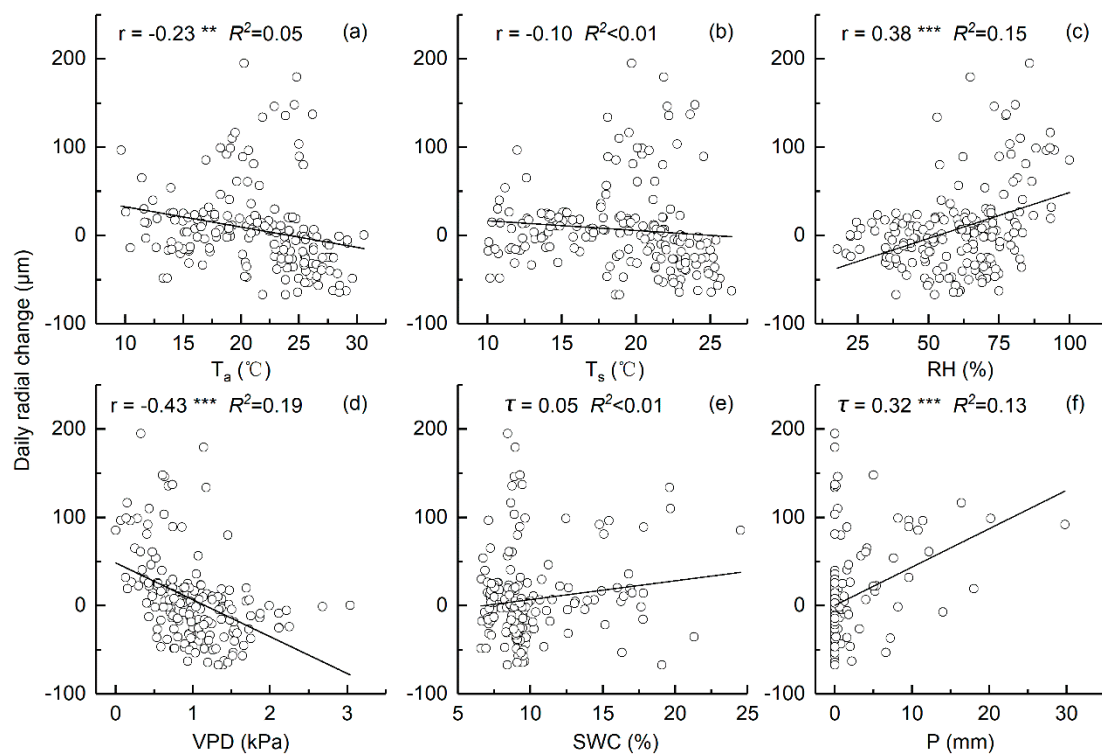


Figure 7. Correlations between DRC of *P. orientalis* and environmental factors of T_a (a), T_s (b), RH (c), VPD (d), SWC (e), and P (f) during growing season. Pearson correlation coefficient (r) and Kendall's tau coefficient (τ) values are shown with *: $p < 0.05$, **: $p < 0.01$, ***: $p < 0.001$.

4. Discussion

4.1. Patterns of Diurnal Stem Cycle

At the daily scale, stem radial variation is closely linked to stem water status [10]. Two opposing daily cycle patterns were observed for *P. orientalis* during warm and cold seasons (Figure 4). A normal diurnal cycle is observed during the warm period (i.e., stage 2, $T_a > 0$ °C). During the daytime, as air temperature rises, tree transpiration increases, and stems shrink due to tree transpiration exceeding water absorption via roots, with internal water reserves in the stem used in transpiration. Following the afternoon, as air temperature decreases, tree transpiration weakens, and stems swell due to excess absorption of water by roots relative to transpiration and refilling of stem water [36]. During the cold period (i.e., stage 1, $T_a < 0$ °C), the rhythm of diurnal stem radial variation exhibits inverted cycles, with night-time shrinkage and daytime swelling. During this stage, transpiration is no longer the primary driver of winter circadian stem cycles [18]. In particular, Zweifel and Hasler [17] proposed a mechanism of “frost shrinkage and thaw expansion” cycles owing to the transport of water between bark and wood that is primarily dependent on air temperatures. In our study, a daily mean air temperature of 0 °C is the critical threshold related to seasonal shifts in stem diurnal cycle patterns. This observation is consistent with a study by Wang [37] within a semi-arid area of northwestern China. The latter study observed that the partitioning between two phases of seasonal stem radial variation for *Sabina przewalskii* Kom. trees was strongly linked to the occurrence of 0 °C daily mean air temperatures.

The daily mean and minimum air temperatures are closely related. When daily mean air temperature fluctuates around 0 °C, daily minimum air temperatures also fluctuate around −5 °C. King et al. [18] proposed that the “frost shrinkage and thaw expansion” cycles are attributable to osmotic water movement due to temperature changes around the freezing point of sap. When air temperatures are below approximately −5 °C, extra-cellular water in the xylem begins to freeze, thereby

inducing the osmotic withdrawal of intra-cellular water from living cells (e.g., mainly bark cells), followed by frost-induced stem shrinkage [18]. Consistent with our results, Zweifel and Hasler [17] also found that normal diurnal cycles of *Picea abies* are quickly replaced by “frost shrinkage and thaw expansion” cycles when daily minimum air temperatures drop below $-5\text{ }^{\circ}\text{C}$.

4.2. Seasonal Patterns of Stem Radius Variation

Clear seasonal variation in patterns of *P. orientalis* stem changes was observed and was affected by environmental factors and especially temperature changes. During spring rehydration (phase A), soil temperatures increase above $0\text{ }^{\circ}\text{C}$, and frozen soils and snow cover begin to melt. Both of these processes lead to increases in SWC values. During water deficits due to winter rehydration, stem tissues complete water recovery via water absorption with roots [20]. Using dendrometer measurements, Zweifel et al. [38] and Wang et al. [37] defined the growing season onset as when stem diameters exceed the maximum value of the previous year, and the season ends when stems exhibit the maximum diameter of the current year. Accordingly, the summer growing season (phase B) is estimated in our study as the period from late-March to late-September. As temperatures gradually increase, trees enter an active growth period under relatively good soil water conditions, wherein obvious stem contractions are mainly influenced by drought. These results are consistent with those of Jiang et al. [11], suggesting that *P. orientalis* stem diameters reach maximum values in late September and then plateau. During autumn stagnation (i.e., phase C), when temperatures decrease, plant transpiration decreases, and stem tissue moisture remains relatively stable. Trees thus enter a stable plateau period in autumn, although lignification of stem tissue cell walls may still occur during this time. However, such processes contribute very little to radial variation [39]. During winter contraction (phase D), when air and soil temperatures drop below $0\text{ }^{\circ}\text{C}$, trees cannot absorb water from frozen soils, and the water stored in stem tissues is used for transpiration, resulting in continuous stem shrinkage [37]. Dehydration and contraction of stems in winter increase cytoplasm concentrations within tissue cells, thereby improving the ability of tissue cells to resist damage from freezing and represent a self-protection survival strategy of trees [17]. Consistent with our results, Wang et al. [37] and Wang et al. [19] also observed that the stem radial variation of *Sabina przewalskii* Kom. and *Picea crassifolia* Kom. enters relatively stable plateaus in autumn and then clearly contracts when the air temperatures drop below $0\text{ }^{\circ}\text{C}$.

Similar seasonal patterns of stem radial variation that are consistent with those of the present study have been previously observed [20,38]. Turcotte et al. [20] defined three distinct seasonal stages of seasonal stem radial variation of black spruce that included winter shrinkage, spring rehydration, and summer transpiration. Zweifel et al. [38] also reported that the stem stagnation period after the growing season is relatively short in alpine treeline areas and that it enters a long-term dehydration stage when air temperatures drop below $0\text{ }^{\circ}\text{C}$ in autumn. However, other results contrast with those reported here. For example, the seasonal stem radial variation of *Pinus pinaster* Ait. in Mediterranean climates exhibits a bimodal distribution, and the stems exhibit sustained contraction in summers due to high temperatures and drought [21]. Furthermore, stem radial variation of *Callitris intratropica* R.T. Baker and H.G. Smith in tropical regions exhibits typical “S” curves due to relatively good soil moisture conditions and the lack of an obvious shrinkage period during the year [22]. The discrepancies among results of this study and others are related to the different climatic conditions of the study areas. Dynamic changes in environmental factors, and especially temperature, influence soil water characteristics of habitats and stem water status that in turn affects the seasonality of stem radial variation.

4.3. Environmental Factors That Influence Daily Stem Variation during Growing Season

During the growing season (phase B), the MDS of *P. orientalis* was positively correlated with T_a . High air temperatures lead to increases in transpiration and required more stem tissue water for transpiration [24], thereby increasing MDS. MDS has been observed as directly correlated with air temperatures in Fino-lemon trees [40], Douglas-fir trees [24], and Norway spruce trees [41]. In addition, MDS was negatively correlated with SWC in this study. These results could be explained by the increase

of water absorption by roots for plant transpiration under higher soil moisture conditions, thereby reducing the amount of stem tissue water required for transpiration and a concomitant reduction in MDS [5,42]. Garnier and Berger [43] observed similar results, wherein drought caused an increase in stem shrinkage. However, the results of Devine and Harrington [24] contrast with ours via the lack of correlation between diurnal stem contraction and SWC during the growing season. These differences may be related to differences in soil water conditions among sites. In the latter study, soil water availability remained relatively high throughout the growing season, and stem tissue water was relatively stable. In contrast, drought in mid-late May and July–August in our study resulted in SWCs generally below 10%, which would cause increased internal stem water to be used for transpiration and consequent MDS increases.

The control of VPD on MDS occurred at a threshold of 0.8 kPa (Figure 6). MDS linearly increased by increasing VPD below the threshold and decreased with increasing VPD above this threshold. Such results could be explained by stomatal closure to limit water loss, given that stomatal conductance is affected by the combined control of VPD and soil moisture [43–45]. The relationship between SWC and VPD in our study was described by exponential functions (Figure 8). When VPD was below 0.8 kPa, plant transpiration enhanced with VPD increases while SWC rapidly decreased, and root water absorption also decreased, leading to the use of more stored stem water for transpiration and therefore increases in MDS. When VPD was above 0.8 kPa, the soil moisture decreased to <10%. With increases in VPD, trees undergo severe water stress and stomatal conductance decreases to prevent excessive water loss, thereby leading to weakening of transpiration and MDS decreases. This process has been observed in some study systems [44,46] but not in many others [24,47,48] that instead observed linear and positive increases of MDS with VPD. These differences primarily depend on the level of plant water stress that is experienced [49], wherein the positive relationships between MDS and VPD were almost always observed under non-limiting soil water availability.

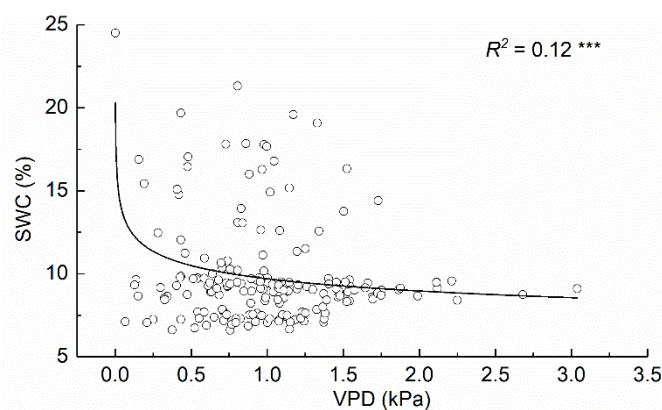


Figure 8. Correlation between the vapor pressure deficit (VPD) and soil water content (SWC) during growing season. *** $p < 0.001$.

The DRC of *P. orientalis* was negatively correlated with T_a during the growing season. Higher air temperatures induce increases in transpiration and cause a decline in soil moisture, thereby intensifying tree water deficits and constricting radial growth [21]. Lower soil moisture conditions and high temperatures led to stem contraction (DCR < 0) in our study, as exemplified during the drought period between mid-late May and July–August, when trees are exposed to severe water stress. Abe et al. [50] and Zweifel et al. [51] reported that growth is slowed or stopped during shrinkage periods since wood formation tends to cease when trees are under water stress for at least several days. Precipitation increases soil water content but also wets crowns, which then reduces the negative pressure in conductance systems and increases the turgor in stem cambial cells, thereby favoring cell division and expansion [11,52]. DRC was positively correlated with RH and negatively correlated with VPD. High RH and low VPD values can lower transpiration and increase stem water status, thereby

promoting radial growth [18]. These results coincide with those of Wang et al. [19] wherein P and RH positively affected the stem growth of Qinghai spruce in a semi-arid area of northwestern China, as observed by dendrometer measurements. Liang et al. [53] also used a dendrochronological approach and observed that monthly P and relative air humidity during the growing season were the primary environmental factors that affected the growth of *Pinus tabulaeformis* trees in semi-arid areas of northern central China.

4.4. Limitations

Based on the 1-year dendrometer monitoring data of four sample trees located on a northern slope, this study illustrated the intra-annual stem radial variation of *P. orientalis* in northern China. The selection of sample trees mainly focused on the average growth but did not relate to differences in age. Oberhuber et al. [41] and Li et al. [54] suggested that there are differences in stem radial variation between trees of different ages. In future research, the number of selected trees should be increased to reveal the difference in stem radial growth of different ages. Using 1 year dendrometer data, the seasonal patterns of stem radius variation obtained in this paper must be verified in the future using long-term monitoring data, because the changes in environmental factors between years will affect the tree growth process. Different habitats, such as different slopes and aspects, have different environmental conditions, which may cause differences in tree radial growth, which should also receive attention in future research.

5. Conclusions

Based on the dendrometer data, this study revealed the daily and seasonal patterns of the stem radial variation of *P. orientalis* in northern China. The diurnal stem cycles were mainly controlled by air temperature, and a daily mean air temperature of 0 °C was a critical threshold that was related to seasonal shifts in stem diurnal cycle patterns, which is only an external phenomenon. The physiological mechanism of air temperature affecting the diurnal cycle patterns must be studied in the future based on a combination of control experiments and field plot monitoring. The environmental factors determined the seasonal patterns of stem radial variation by affecting the seasonal changes of stem water status. During the growing season, daily stem variations (MDS and DRC) were closely related to the water status of stem tissues. Environmental factors, such as T_a , RH, VPD, and SWC, influenced the stem growth by affecting stem water condition. As the temperature rises, the climate in northern China will show a trend of drought in the future [55]. *P. orientalis* will face more severe drought stress, and the radial growth of trees could be inhibited. Some regions may not be suitable for the survival of *P. orientalis*. Under increasingly dry conditions, how the stem water content changes on the daily and seasonal scales will have an impact, and thus affect stem growth. Thus, in future research, it will be necessary to strengthen the monitoring of stem water status of trees, including MDS, sap flow, leaf water potential, and other indicators related to tissue moisture. Meanwhile, combined with long-term dendrometer monitoring data, studying the response of radial growth for *P. orientalis* to climate change is necessary for the management of ecological restoration in the arid regions of northern China.

Author Contributions: Conceptualization, Y.J., and M.D.; investigation, M.D., B.W., and X.D.; formal analysis, M.D. and B.W.; writing—original draft preparation, M.D. and B.W.; writing—review and editing, M.D., B.W., and Y.J.; funding acquisition, Y.J., and M.D.

Funding: This research was funded by the National Natural Science Foundation of China (Grant Nos. 41630750, 41771051, 41601198, 41401061).

Acknowledgments: We thank Mingchang Wang, Biao Wang and Hui Wang for their help in the field investigation.

Conflicts of Interest: The authors declare no conflict of interest.

References

1. Zhang, R.B.; Yuan, Y.J.; Gou, X.H.; Zhang, T.W.; Zou, C.; Ji, C.R.; Fan, Z.A.; Qin, L.; Shang, H.M.; Li, X.J. Intra-annual radial growth of Schrenk spruce (*Picea schrenkiana* Fisch et Mey) and its response to climate on the northern slopes of the Tianshan mountains. *Dendrochronologia* **2016**, *40*, 36–42. [[CrossRef](#)]
2. Fritts, H.C.; Shatz, D.J. Selecting and characterizing tree-ring chronologies for dendroclimatic analysis. *Tree-Ring Bull.* **1975**, *35*, 31–46.
3. Gutierrez, E.; Campelo, F.; Julio Camarero, J.; Ribas, M.; Muntan, E.; Nabais, C.; Freitas, H. Climate controls act at different scales on the seasonal pattern of *Quercus ilex* L. stem radial increments in NE Spain. *Trees* **2011**, *25*, 637–646. [[CrossRef](#)]
4. Perez, C.A.; Carmona, M.R.; Aravena, J.C.; Farina, J.M.; Armesto, J.J. Environmental controls and patterns of cumulative radial increment of evergreen tree species in montane, temperate rainforests of Chiloe Island, southern Chile. *Austral Ecol.* **2009**, *34*, 259–271. [[CrossRef](#)]
5. Liu, Z.B.; Wang, Y.H.; Tian, A.; Yu, P.T.; Xiong, W.; Xu, L.H.; Wang, Y.R. Intra-annual variation of stem radius of *Larix principis-rupprechtii* and its response to environmental factors in Liupan mountains of Northwest China. *Forests* **2017**, *8*, 382. [[CrossRef](#)]
6. Tian, Q.Y.; He, Z.B.; Xiao, S.C.; Peng, X.M.; Ding, A.J.; Lin, P.F. Response of stem radial growth of Qinghai spruce (*Picea crassifolia*) to environmental factors in the Qilian Mountains of China. *Dendrochronologia* **2017**, *44*, 76–83. [[CrossRef](#)]
7. Liu, X.S.; Nie, Y.Q.; Wen, F. Seasonal dynamics of stem radial increment of *Pinus taiwanensis* Hayata and its response to environmental factors in the Lushan mountains, Southeastern China. *Forests* **2018**, *9*, 387. [[CrossRef](#)]
8. Downes, G.; Beadle, C.; Worledge, D. Daily stem growth patterns in irrigated *Eucalyptus globulus* and *E. nitens* in relation to climate. *Trees* **1999**, *14*, 102–111. [[CrossRef](#)]
9. Dong, M.Y.; Jiang, Y.; Zhang, W.T.; Yang, Y.G.; Yang, H.C. Effect of alpine treeline conditions on the response of the stem radial variation of *Picea Meyer* Reb. Et Wils to environmental factors. *Pol. J. Ecol.* **2011**, *59*, 729–739.
10. Drew, D.M.; Downes, G.M. The use of precision dendrometers in research on daily stem size and wood property variation: A review. *Dendrochronologia* **2009**, *27*, 159–172. [[CrossRef](#)]
11. Jiang, Y.; Wang, B.Q.; Dong, M.Y.; Huang, Y.M.; Wang, M.C.; Wang, B. Response of daily stem radial growth of *Platycladus orientalis* to environmental factors in a semi-arid area of North China. *Trees* **2015**, *29*, 87–96. [[CrossRef](#)]
12. Sprengel, L.; Stangler, D.F.; Sheppard, J.; Morhart, C.; Spiecker, H. Comparative analysis of the effects of stem height and artificial pruning on seasonal radial growth dynamics of Wild Cherry (*Prunus avium* L.) and Sycamore (*Acer pseudoplatanus* L.) in a widely spaced system. *Forests* **2018**, *9*, 174. [[CrossRef](#)]
13. Makinen, H.; Seo, J.-W.; Nojd, P.; Schmitt, U.; Jalkanen, R. Seasonal dynamics of wood formation: A comparison between pinning, microcoring and dendrometer measurements. *Eur. J. For. Res.* **2008**, *127*, 235–245. [[CrossRef](#)]
14. Bräuning, A.; Volland-Voigt, F.; Burchardt, I.; Ganzhi, O.; Nauss, T.; Peters, T. Climatic control of radial growth of *Cedrela montana* in a humid mountain rainforest in Southern Ecuador. *Erdkunde* **2009**, *63*, 337–345. [[CrossRef](#)]
15. Urrutia-Jalabert, R.; Rossi, S.; Deslauriers, A.; Malhi, Y.; Lara, A. Environmental correlates of stem radius change in the endangered *Fitzroya cupressoides* forests of southern Chile. *Agric. For. Meteorol.* **2015**, *200*, 209–221. [[CrossRef](#)]
16. Coccozza, C.; Tognetti, R.; Giovannelli, A. High-resolution analytical approach to describe the sensitivity of tree-environment dependences through stem radial variation. *Forests* **2018**, *9*, 134. [[CrossRef](#)]
17. Zweifel, R.; Hasler, R. Frost-induced reversible shrinkage of bark of mature subalpine conifers. *Agric. For. Meteorol.* **2000**, *102*, 213–222. [[CrossRef](#)]
18. King, G.; Fonti, P.; Nievergelt, D.; Buntgen, U.; Frank, D. Climatic drivers of hourly to yearly tree radius variations along a 6 degrees C natural warming gradient. *Agric. For. Meteorol.* **2013**, *168*, 36–46. [[CrossRef](#)]
19. Wang, W.B.; Zhang, F.; Yuan, L.M.; Wang, Q.T.; Zheng, K.; Zhao, C.Y. Environmental factors effect on stem radial variations of *Picea crassifolia* in Qilian Mountains, Northwestern China. *Forests* **2016**, *7*, 210. [[CrossRef](#)]

20. Turcotte, A.; Morin, H.; Krause, C.; Deslauriers, A.; Thibeault-Martel, M. The timing of spring rehydration and its relation with the onset of wood formation in black spruce. *Agric. For. Meteorol.* **2009**, *149*, 1403–1409. [[CrossRef](#)]
21. Vieira, J.; Rossi, S.; Campelo, F.; Freitas, H.; Nabais, C. Seasonal and daily cycles of stem radial variation of *Pinus pinaster* in a drought-prone environment. *Agric. For. Meteorol.* **2013**, *180*, 173–181. [[CrossRef](#)]
22. Drew, D.M.; Richards, A.E.; Cook, G.D.; Downes, G.M.; Gill, W.; Baker, P.J. The number of days on which increment occurs is the primary determinant of annual ring width in *Callitris intratropica*. *Trees* **2013**, *28*, 31–40. [[CrossRef](#)]
23. Tardif, J.; Flannigan, M.; Bergeron, Y. An analysis of the daily radial activity of 7 boreal tree species, northwestern Quebec. *Environ. Monit. Assess.* **2001**, *67*, 141–160. [[CrossRef](#)] [[PubMed](#)]
24. Devine, W.D.; Harrington, C.A. Factors affecting diurnal stem contraction in young Douglas-fir. *Agric. For. Meteorol.* **2011**, *151*, 414–419. [[CrossRef](#)]
25. Tian, Y.; Zhang, Q.L.; Liu, X.; Meng, M. The relationship between stem diameter shrinkage and tree bole moisture loss due to transpiration. *Forests* **2019**, *10*, 290. [[CrossRef](#)]
26. Jimenez, M.N.; Navarro, F.B.; Sanchez-Miranda, A.; Ripoll, M.A. Using stem diameter variations to detect and quantify growth and relationships with climatic variables on a gradient of thinned Aleppo pines. *For. Ecol. Manag.* **2019**, *442*, 53–62. [[CrossRef](#)]
27. Oberhuber, W.; Gruber, A.; Kofler, W.; Swidrak, I. Radial stem growth in response to microclimate and soil moisture in a drought-prone mixed coniferous forest at an inner Alpine site. *Eur. J. For. Res.* **2014**, *133*, 467–479. [[CrossRef](#)] [[PubMed](#)]
28. Hu, X.G.; Wang, T.L.; Liu, S.S.; Jiao, S.Q.; Jia, K.H.; Zhou, S.S.; Jin, Y.Q.; Li, Y.; El-Kassaby, Y.A.; Mao, J.F. Predicting future seed sourcing of *Platycladus orientalis* (L.) for future climates using climate niche models. *Forests* **2017**, *8*, 471. [[CrossRef](#)]
29. Huang, R.F.; Zhao, Y.K.; Lv, J.X.; Bao, F.C. Response of ring width and ring density of *Platycladus orientalis* to climate change in Beijing. *Sci. Silv. Sin.* **2006**, *42*, 78–82. (In Chinese)
30. Lu, W.W.; Yu, X.X.; Jia, G.D.; Li, H.Z.; Liu, Z.Q. Responses of intrinsic water-use efficiency and tree growth to climate change in semi-arid areas of North China. *Sci. Rep.* **2018**, *8*, 308.
31. Ziaco, E.; Biondi, F. Stem circadian phenology of four pine species in naturally contrasting climates from sky-island forests of the Western USA. *Forests* **2018**, *9*, 396. [[CrossRef](#)]
32. Murray, F.W. On the computation of saturation vapor pressure. *J. Appl. Meteorol.* **1967**, *6*, 203–204. [[CrossRef](#)]
33. Deslauriers, A.; Rossi, S.; Anfodillo, T. Dendrometer and intra-annual tree growth: What kind of information can be inferred? *Dendrochronologia* **2007**, *25*, 113–124. [[CrossRef](#)]
34. Oberhuber, W. Soil water availability and evaporative demand affect seasonal growth dynamics and use of stored water in co-occurring saplings and mature conifers under drought. *Trees* **2017**, *31*, 467–478. [[CrossRef](#)] [[PubMed](#)]
35. Duchesne, L.; Houle, D. Modelling day-to-day stem diameter variation and annual growth of balsam fir (*Abies balsamea* (L.) Mill.) from daily climate. *For. Ecol. Manag.* **2011**, *262*, 863–872. [[CrossRef](#)]
36. Deslauriers, A.; Morin, H.; Urbinati, C.; Carrer, M. Daily weather response of balsam fir (*Abies balsamea* (L.) Mill.) stem radius increment from dendrometer analysis in the boreal forests of Québec (Canada). *Trees* **2003**, *17*, 477–484. [[CrossRef](#)]
37. Wang, Z.Y.; Yang, B.; Deslauriers, A.; Qin, C.; He, M.H.; Shi, F.; Liu, J.J. Two phases of seasonal stem radius variations of *Sabina przewalskii* Kom. in northwestern China inferred from sub-diurnal shrinkage and expansion patterns. *Trees* **2012**, *26*, 1747–1757. [[CrossRef](#)]
38. Zweifel, R.; Eugster, W.; Etzold, S.; Dobbertin, M.; Buchmann, N.; Haesler, R. Link between continuous stem radius changes and net ecosystem productivity of a subalpine Norway spruce forest in the Swiss Alps. *New Phytol.* **2010**, *187*, 819–830. [[CrossRef](#)] [[PubMed](#)]
39. He, M.H.; Yang, B.; Wang, Z.Y.; Bräuning, A.; Pourtahmasi, K.; Oladi, R. Climatic forcing of xylem formation in Qilian juniper on the northeastern Tibetan Plateau. *Trees* **2016**, *30*, 923–933. [[CrossRef](#)]
40. Ortuno, M.F.; Garcia-Orellana, Y.; Conejero, W.; Ruiz-Sanchez, M.C.; Mounzer, O.; Alarcon, J.J.; Torrecillas, A. Relationships between climatic variables and sap flow, stem water potential and maximum daily trunk shrinkage in lemon trees. *Plant Soil* **2006**, *279*, 229–242. [[CrossRef](#)]
41. Oberhuber, W.; Hammerle, A.; Kofler, W. Tree water status and growth of saplings and mature Norway spruce (*Picea abies*) at a dry distribution limit. *Front. Plant Sci.* **2015**, *6*, 703. [[CrossRef](#)] [[PubMed](#)]

42. Barraclough, A.D.; Zweifel, R.; Cusens, J.; Leuzinger, S. Daytime stem swelling and seasonal reversal in the peristaltic depletion of stored water along the stem of *Avicennia marina* (Forssk.) Vierh. *Tree Physiol.* **2018**, *38*, 965–978. [[CrossRef](#)] [[PubMed](#)]
43. Garnier, E.; Berger, A. Effect of water stress on stem diameter changes of Peach trees growing in the field. *J. Appl. Ecol.* **1986**, *23*, 193–209. [[CrossRef](#)]
44. Hinckley, T.M.; Bruckerhoff, D.N. Effects of drought on water relations and stem shrinkage of *Quercus alba*. *Can. J. Bot.* **1975**, *53*, 62–72. [[CrossRef](#)]
45. Grossiord, C.; Sevanto, S.; Borrego, I.; Chan, A.M.; Collins, A.D.; Dickman, L.T.; Hudson, P.J.; McBranch, N.; Michaletz, S.T.; Pockman, W.T.; et al. Tree water dynamics in a drying and warming world. *Plant Cell Environ.* **2017**, *40*, 1861–1873. [[CrossRef](#)] [[PubMed](#)]
46. Mei, T.T.; Fang, D.M.; Roll, A.; Niu, F.R.; Hendrayanto; Holscher, D. Water use patterns of four tropical bamboo species assessed with sap flux measurements. *Front. Plant Sci.* **2015**, *6*, 1202.
47. Moriana, A.; Moreno, F.; Giron, I.F.; Conejero, W.; Ortuno, M.F.; Morales, D.; Corell, M.; Torrecillas, A. Seasonal changes of maximum daily shrinkage reference equations for irrigation scheduling in olive trees: Influence of fruit load. *Agric. Water Manag.* **2011**, *99*, 121–127. [[CrossRef](#)]
48. Galindo, A.; Rodriguez, P.; Mellisho, C.D.; Torrecillas, E.; Moriana, A.; Cruz, Z.N.; Conejero, W.; Moreno, F.; Torrecillas, A. Assessment of discretely measured indicators and maximum daily trunk shrinkage for detecting water stress in pomegranate trees. *Agric. For. Meteorol.* **2013**, *180*, 58–65. [[CrossRef](#)]
49. Intrigliolo, D.S.; Castel, J.R. Evaluation of grapevine water status from trunk diameter variations. *Irrig. Sci.* **2007**, *26*, 49–59. [[CrossRef](#)]
50. Abe, H.; Nakai, T.; Utsumi, Y.; Kagawa, A. Temporal water deficit and wood formation in *Cryptomeria japonica*. *Tree Physiol.* **2003**, *23*, 859–863. [[CrossRef](#)]
51. Zweifel, R.; Haeni, M.; Buchmann, N.; Eugster, W. Are trees able to grow in periods of stem shrinkage? *New Phytol.* **2016**, *211*, 839–849. [[CrossRef](#)] [[PubMed](#)]
52. Köcher, P.; Horna, V.; Leuschner, C. Environmental control of daily stem growth patterns in five temperate broad-leaved tree species. *Tree Physiol.* **2012**, *32*, 1021–1032. [[CrossRef](#)] [[PubMed](#)]
53. Liang, E.Y.; Eckstein, D.; Liu, H.Y. Climate-growth relationships of relict *Pinus tabulaeformis* at the northern limit of its natural distribution in northern China. *J. Veg. Sci.* **2008**, *19*, 393–406. [[CrossRef](#)]
54. Li, X.X.; Liang, E.Y.; Gričar, J.; Prislán, P.; Rossi, S.; Čufar, K. Age dependence of xylogenesis and its climatic sensitivity in Smith fir on the south-eastern Tibetan Plateau. *Tree Physiol.* **2013**, *33*, 48–56. [[CrossRef](#)] [[PubMed](#)]
55. Hu, S.; Mo, X.G.; Lin, Z.H. Projections of spatial-temporal variation of drought in north China. *Arid Land Geogr.* **2015**, *38*, 239–248. (In Chinese)

